Performance Analysis of Optical Synchronous CDMA Communication Systems with PPM Signaling

Hossam M. H. Shalaby, *Member, IEEE*

Abstract—**Direct-detection optical synchronous code-division multiple-access (CDMA) systems with M-ary pulse-position modulation (PPM) signaling are investigated. Optical orthogonal codes are used as the signature sequences of our system. A union upper bound on the bit error rate is derived taking into account the effect of the background noise, multiple-user interference, and receiver shot noise. The performance characteristics are then discussed for a variety of system parameters. Another upper bound on the probability of error is also obtained (based on Chernoff inequality). This bound is utilized to derive achievable expressions for both the maximum number of users that can communicate simultaneously with asymptotically zero error rate and the channel capacity. Our results show that under average power and bit error rate constraints, there always exists a pulse position multiplicity that permit all the subscribers to communicate simultaneously.**

I. INTRODUCTION

Optical code-division multiple-access (CDMA) systems have been given an increasing interest in the recent years [1–11]. This is due to the vast bandwidth offered by the optical links and the extra-high *optical* signal processing speed offered by the optical components. As a result, Optical CDMA can accommodate a larger number of simultaneous users than the radio-frequency techniques.

Most work done on optical CDMA has concentrated on the binary transmission of data, e.g., on-off keying (OOK). Very few suggested using M-ary transmission of data [6,7]. Lam and Hussain [6], for example, suggested an M-ary system in which each symbol is represented by one of M mutually orthogonal sequences (signatures). Thus a total of MN code sequences are required, where N is the number of users. In [7], Dale and Gagliardi suggested encoding the symbols using M-ary pulse-position modulation (PPM) format and then transmitting an aperiodic signature in place of the PPM pulse. In their analysis, Dale and Gagliardi assumed that the photodetector shot noise, dark current, and thermal noise can be modeled as Gaussian random processes. They showed that under fixed bit rate and chip time, there is no advantage in using PPM.

Paper approved by Paul R. Prucnal, the Editor for Lightwave Networks of the IEEE Communications Society. Manuscript received July 15, 1993; revised August 15, 1994. This paper was presented in part at the IEEE Global Telecommunications Conference (GLOBECOM '93), Houston, Texas, November 29–December 2, 1993.

The author is with the Department of Electrical Engineering, Faculty of Engineering, University of Alexandria, Alexandria 21544, Egypt.

IEEE Log Number 9410095.

0090-6778/95$4.00

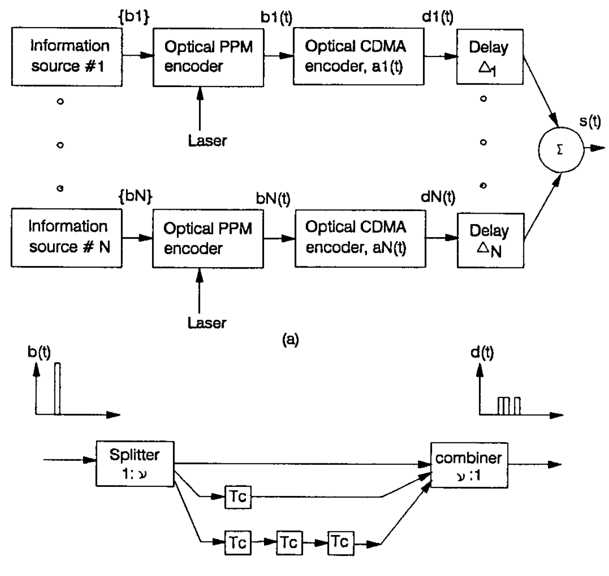

Fig. 1. (a) Optical CDMA system with PPM signaling. (b) An example of optical CDMA encoder for one of the sources.

On the other hand, they showed that PPM is superior to OOK if the average power rather than the chip time is the constraining factor.

We have two main objectives in this paper. Our first aim is to investigate the performance of direct-detection optical M-ary PPM-CDMA communication systems under the assumption of Poisson shot noise model for the receiver photodetector and synchronization between the users' symbols. Our second aim is to derive an asymptotic relation between the optimum number of simultaneous users and the pulse position multiplicity.

In PPM signaling format, each symbol is represented by a single laser pulse positioned in one of M (disjoint) possible time slots. The width of each slot is τ seconds. The entire symbol thus extends over a time frame of $T = M\tau$ seconds. This signaling format is attractive in optical communications because of its simple implementation and efficient use of the available source energy [13–15].

The model for an optical PPM-CDMA communication system is shown in Figs. 1 and 2. The transmitter in Fig. 1 is composed of N simultaneous users. Each user transmits M-ary continuous data symbols. The output symbol of the kth information source modulates the position of a

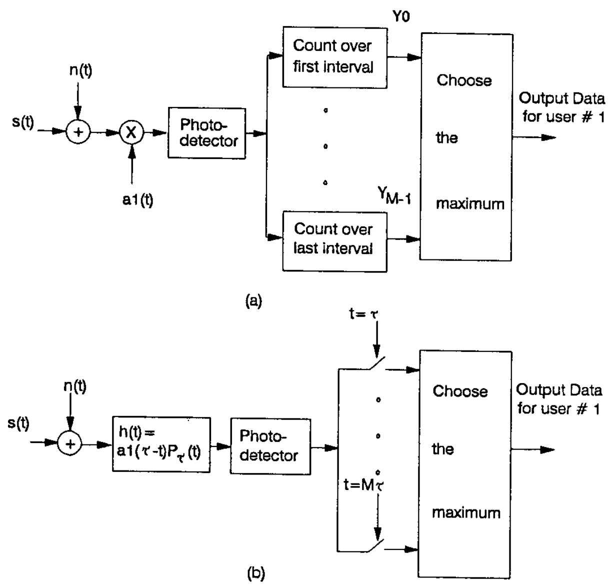

Fig. 2. Direct-detection optical PPM-CDMA system model: (a) Using an optical correlator. (b) Using an optical matched filter.

laser pulse to form the PPM signal. This signal is then multiplied by a spreading sequence $a^k(t)$, which characterizes the kth user. The output waveform is finally transmitted over the optical channel. In asynchronous CDMA each optical signal is time delayed by Δ_k with respect to a reference instant $t = 0$. In synchronous CDMA, however, there are no time delays among the signals, $\Delta_k = 0$. An equivalent all-optical multiplier [3,6] is shown in Fig. 1(b) which is just a tapped optical delay line [12]. At the receiving end, the received optical signal (composed of the sum of the N delayed users' optical signals in addition to the background noise) is multiplied by the same sequence $a^k(t)$ and, Fig. 2 (a), then converted using the photodetector into an electric signal which is passed to the PPM decoder to obtain the data. The PPM decoder is just a comparison between the photon counts over the M time slots: the number of the slot with the greatest count is declared to be the transmitted symbol. To make full use of the vast bandwidth available to the optical network, an equivalent all-optical receiver is shown in Fig. 2(b), where the received optical signal is passed to a matched filter with impulse response

$$h(t) = a^k(\tau - t)P_\tau(t) ,$$

where $P_\tau(\cdot)$ is a rectangular pulse of duration τ:

$$P_\tau(t) \stackrel{\text{def}}{=} \begin{cases} 1 ; & \text{if } 0 < t < \tau, \\ 0 ; & \text{otherwise.} \end{cases}$$

The output of the matched filter is then photodetected and finally sampled at M different instants $\{\tau, 2\tau, \ldots, M\tau\}$ to provide the photon counts over the M time slots.

The rest of the paper is organized as follows: Section II is devoted for the derivation of the bit error probabilities. In Section III we present some numerical results where we investigate the effect of some parameters (the background noise, the number of users, the pulse-position multiplicity, etc.) on the performance of the optical PPM-CDMA system. In Section IV we obtain an asymptotically ($M \to \infty$) achievable expression of the maximum number of users that can be accommodated by the system so that the bit error rate is asymptotically zero. Finally, we give our conclusion in Section V.

II. Bit Error Rate of the Optical PPM-CDMA Systems

We assume that each user is assigned an optical code sequence (or signature sequence) of length L and weight ν. That is the kth user is assigned the code sequence $(a_0^k, \ldots, a_{L-1}^k)$, where $a_i^k \in \{0, 1\}$ and the number of i's with $a_i^k = 1$ equals ν. The spreading signature waveform, $a^k(t)$, is assumed to be periodic of period τ (the slot width), hence it can be written as

$$a^k(t) = \sum_{i=-\infty}^{\infty} a_i^k P_{T_c}(t - iT_c) ,$$

where $a_{i+L}^k = a_i^k$ for all integers i, $T_c = \tau/L$ is the chip time, and $P_{T_c}(\cdot)$ was defined previously. The kth information source generates the data sequence $\{b_j^k\}_{j=-\infty}^{\infty}$, where $b_j^k \in \{0, \ldots, M-1\}$. This sequence modulates the position of a laser pulse so that the output of the optical PPM encoder can be written as

$$b^k(t) = \sum_{j=-\infty}^{\infty} \lambda_s P_\tau(t - b_j^k \tau - jT) ,$$

where λ_s is the signal photon rate (which is assumed to be constant for all the transmitters) and T is the PPM time frame defined previously. This PPM signal is then multiplied by $a^k(t)$ to give the baseband signal of the kth user:

$$d^k(t) = b^k(t)a^k(t) .$$

We assume that the kth signal is associated with a delay Δ_k (which is zero in the case of synchronous transmitters). Hence the total signal waveform can be written as

$$s(t) = \sum_{k=1}^{N} d^k(t - \Delta_k) ,$$

where N is the number of simultaneous users. The received waveform at the front end of each receiver is thus

$$r(t) = s(t) + n(t) ,$$

where $n(t)$ is the optical background noise. The input to the photodetector of user 1, Fig. 2(a), is thus given by

$$\begin{aligned} y(t) &= r(t)a^1(t - \Delta_1) \\ &= [a^1(t - \Delta_1)]^2 b^1(t - \Delta_1) + a^1(t - \Delta_1)n(t) \\ &\quad + \sum_{k=2}^{N} a^1(t - \Delta_1)a^k(t - \Delta_k)b^k(t - \Delta_k) . \end{aligned}$$

The first term in the last equation is the desired signal, the second term is due to the background noise, and the last term is due to the interference from other users. Since we are dealing with direct (noncoherent) detection, the optical signals and the optical noise are additive in intensity. The photon count over the ith slot of the kth user can be modeled as a conditional Poisson random variable Y_i^k [13]. Thus for the first user:

$$(\forall i \in \{0,\ldots,M-1\}) \qquad Y_i = Z_i + W_i + I_i \ ,$$

where we have assumed for simplicity that $Y_i^1 = Y_i$. Here W_i is a Poisson photon count due to the background noise. Z_i and I_i are conditionally independent Poisson photon counts given $\{b_j^k\}$ and $\{\Delta_k\}$ due to the desired signal and the multiple-user interference, respectively. To obtain the conditional mean of Y_i, we evaluate the conditional expectation of each of the three photon counts composing it. Denoting the background noise photon rate by λ_0, it is easy to see that

$$E[W_i] = \nu\lambda_0 T_c \ .$$

The Poisson random variable Z_i depends only on b_0^1 and Δ_1. Hence its conditional mean value is given by

$$\begin{aligned} E[Z_i|\Delta_1, b_0^1] &= \int_{\Delta_1+i\tau}^{\Delta_1+(i+1)\tau} [a^1(t-\Delta_1)]^2 b^1(t-\Delta_1)dt \\ &= \int_{\Delta_1+i\tau}^{\Delta_1+(i+1)\tau} \lambda_s [a^1(t-\Delta_1)]^2 \\ &\qquad \times \sum_{j=-\infty}^{\infty} P_\tau(t-\Delta_1-b_j^1\tau-jT)dt \ . \end{aligned}$$

Whence

$$E[Z_i|\Delta_1, b_0^1] = \begin{cases} \nu\lambda_s T_c \ ; & \text{if } b_0^1 = i, \\ 0 \ ; & \text{otherwise.} \end{cases}$$

The conditional mean of the random variable I_i given delays $\Delta \stackrel{\text{def}}{=} \{\Delta_k\}_2^N$ and data symbols $b \stackrel{\text{def}}{=} \{b_{-1}^k, b_0^k\}_{k=2}^N$ can be written as

$$\begin{aligned} &E[I_i|\Delta, b] \\ &= \sum_{k=2}^{N} \int_{\Delta_1+i\tau}^{\Delta_1+(i+1)\tau} a^1(t-\Delta_1)a^k(t-\Delta_k)b^k(t-\Delta_k)dt \\ &= \lambda_s \sum_{k=2}^{N} \int_{\Delta_1+i\tau}^{\Delta_1+(i+1)\tau} a^1(t-\Delta_1)a^k(t-\Delta_k) \\ &\qquad \times \sum_{j=-1}^{0} P_\tau(t-\Delta_k-b_j^k\tau-jT)dt \ . \end{aligned}$$

At this point we assume synchronous CDMA (at both data and chip levels). Hence the delays Δ_k are equal to zero. The random variable I_i now depends only on the symbols $\{b_0^k\}_{k=2}^N$. Substituting into the last equation, yields

$$E[I_i|\{b_0^k\}_{=2}^N] = \lambda_s \sum_{k=2}^{N} \int_{i\tau}^{(i+1)\tau} a^1(t)a^k(t)P_\tau(t-b_0^k\tau-jT)dt \ .$$

Let

$$I_i \stackrel{\text{def}}{=} \sum_{k=2}^{N} I_i^k \ , \tag{1}$$

where I_i^k is the interference in ith interval due to the kth user. This is a conditional Poisson random variable (given b_0^k) with expectation:

$$\begin{aligned} E[I_i^k|b_0^k] &= \lambda_s \int_{i\tau}^{(i+1)\tau} a^1(t)a^k(t)P_\tau(t-b_0^k\tau-jT)dt \\ &= \begin{cases} C_{1k}\lambda_s T_c \ ; & \text{if } b_0^k = i, \\ 0 \ ; & \text{otherwise} \end{cases} \\ &= C_{1k}\lambda_s T_c \delta_{b_0^k,i} \ , \end{aligned}$$

where $\delta_{b_0^k,i}$ is the Kronecker delta and C_{1k} denotes the cross-correlation between the first and kth codes. In the remaining analysis we employ the optical orthogonal codes (OOC's) [10,11] as our typical signature code sequences. OOC's with periodic cross-correlations and out-of-phase periodic auto-correlations bounded by one have been extensively studied in [10]. It has been shown that the maximum number of codes (subscribers) is at most $\frac{L-1}{\nu(\nu-1)}$. OOC's with cross-correlations larger than one can be found in [8,11]. In this case the maximum number of codes can reach $\frac{(L-1)(L-2)}{\nu(\nu-1)(\nu-2)}$ if the auto- and cross-correlations are bounded by two. Thus for OOC's with cross-correlations bounded by one, we have

$$(\forall k, l \in \{1,\ldots,N\},\ k \neq l) \qquad C_{kl} \leq 1 \ .$$

Assume, for simplicity, $C_{1k} = 1$ for every $k \in \{2,\ldots,N\}$ (worst case conditions). Hence

$$E[I_i^k|b_0^k] = \lambda_s T_c \delta_{b_0^k,i} \ .$$

Substituting in (1) yields

$$E[I_i|\{b_0^k\}_{k=2}^N] = \lambda_s T_c \sum_{k=2}^{N} \delta_{b_0^k,i} \ .$$

Define the following set of random variables

$$\kappa_i \stackrel{\text{def}}{=} \sum_{k=2}^{N} \delta_{b_0^k,i}, \qquad i \in \{0,\ldots,M-1\} \ .$$

The random variable κ_i represents the number of optical pulses that cause interference to slot i of the desired user. We notice that each κ_i is a binomial random variable, i.e.,

$$(\forall l \in \{0,\ldots,N-1\}) \quad \Pr\{\kappa_i = l\} = \binom{N-1}{l}\left(\frac{1}{M}\right)^l\left(1-\frac{1}{M}\right)^{N-1-l} \ .$$

Moreover, denote the vector $(\kappa_0,\ldots,\kappa_{M-1})$ by κ. It is easy to check that κ is a multinominal random vector with probability

$$\Pr\{\kappa = (l_0,\ldots,l_{M-1})\} = \frac{1}{M^{N-1}} \cdot \frac{(N-1)!}{l_0!l_1!\ldots l_{M-1}!} \ , \tag{2}$$

where $\sum_{i=0}^{M-1} l_i = N-1$. Assuming equally likely data symbols, we employ the following decision rule: Symbol i is chosen if $Y_i > Y_j$ for every $j \neq i$. If $Y_i = Y_j$, some j's$\neq i$, a random choice between these symbols is made. The probability of a correct decision can thus be lower bounded by:

$$P_C \geq \sum_{i=0}^{M-1} \Pr\{Y_i > Y_0, \ldots, Y_{i-1}, Y_{i+1}, \ldots, Y_{M-1} | b_0^1 = i\} \times \Pr\{b_0^1 = i\}$$
$$= \Pr\{Y_0 > Y_1, \ldots, Y_{M-1} | b_0^1 = 0\}$$
$$= \sum_{l_0=0}^{N-1} \sum_{l_1=0}^{N-1-l_0} \cdots \sum_{l_{M-1}=0}^{N-1-l_0-\cdots-l_{M-2}} \Pr\{Y_0 > Y_1, \ldots, Y_{M-1} | b_0^1 = 0, \kappa = l\} \Pr\{\kappa = l\} , \quad (3)$$

where $l \stackrel{\text{def}}{=} (l_0, \ldots, l_{M-1})$ and

$$\Pr\{Y_0 > Y_1, \ldots, Y_{M-1} | b_0^1 = 0, \kappa = l\} = \sum_{k=0}^{\infty} e^{-(K_s + K_b + \lambda_s T_c l_0)} \frac{(K_s + K_b + \lambda_s T_c l_0)^k}{k!} \times \prod_{j=1}^{M-1} \left[\sum_{i=0}^{k-1} e^{-(K_b + \lambda_s T_c l_j)} \frac{(K_b + \lambda_s T_c l_j)^i}{i!}\right] , \quad (4)$$

where we have defined

$$K_s \stackrel{\text{def}}{=} E[Z_0 | b_0^1 = 0, \kappa = l] = E[Z_0 | b_0^1 = 0] = \nu \lambda_s T_c ,$$
$$K_b \stackrel{\text{def}}{=} E[W_i | b_0^1 = 0, \kappa = l] = E[W_i] = \nu \lambda_0 T_c , \quad (5)$$

and we have used the identity

$$E[I_i | b_0^1 = 0, \kappa = l] = E[I_i | \kappa_i = l_i] = \lambda_s T_c l_i . \quad (6)$$

Here K_s and K_b denote the average photon counts per symbol due to the signal and noise, respectively. Using the relation $P_E = 1 - P_C$, we can obtain an upper bound on the word error probability, P_E. Finally, the equivalent bit error probability P_b can be found from the fact that $P_b = \frac{M/2}{M-1} P_E$ [13, Chap. 8].

III. Numerical Results

It is too expensive to perform numerical calculations using the expressions derived in the previous section especially for large values of M. We thus employ a union bound on the error rate to simplify the calculations. Using (3) we can write

$$P_E \leq 1 - \Pr\{Y_0 > Y_1, \ldots, Y_{M-1} | b_0^1 = 0\}$$
$$\leq \sum_{i=1}^{M-1} \Pr\{Y_i \geq Y_0 | b_0^1 = 0\}$$
$$= (M-1) \Pr\{Y_1 \geq Y_0 | b_0^1 = 0\}$$
$$= (M-1) \times \sum_{l_0=0}^{N-1} \sum_{l_1=0}^{N-1-l_0} \Pr\{Y_1 \geq Y_0 | b_0^1 = 0, \kappa_0 = l_0, \kappa_1 = l_1\} \times \Pr\{\kappa_0 = l_0, \kappa_1 = l_1\} ,$$

where

$$\Pr\{\kappa_0 = l_0, \kappa_1 = l_1\} \stackrel{\text{def}}{=} \sum_{l_2, \ldots, l_{M-1}} \Pr\{\kappa = (l_0, \ldots, l_{M-1})\}$$
$$= \binom{N-1}{l_0} \left(\frac{1}{M}\right)^{l_0} \left(1 - \frac{1}{M}\right)^{N-1-l_0} \times \binom{N-1-l_0}{l_1} \left(\frac{1}{M-1}\right)^{l_1} \left(1 - \frac{1}{M-1}\right)^{N-1-l_0-l_1}$$
$$= \frac{(N-1)!}{l_0! l_1! (N-1-l_0-l_1)!} \cdot \frac{(M-2)^{N-1-l_0-l_1}}{M^{N-1}} ,$$

$$\Pr\{Y_1 \geq Y_0 | b_0^1 = 0, \kappa_0 = l_0, \kappa_1 = l_1\} = \sum_{k=0}^{\infty} e^{-(K_b + \lambda_s T_c l_1)} \frac{(K_b + \lambda_s T_c l_1)^k}{k!} \times \left[\sum_{i=0}^{k} e^{-(K_s + K_b + \lambda_s T_c l_0)} \frac{(K_s + K_b + \lambda_s T_c l_0)^i}{i!}\right] ,$$

and K_s, K_b are as given in (5).

In our numerical evaluations we assume that the rate of data bits (throughput) is fixed at R_0. Normalizing the slot-width with each different value of M is thus mandatory. Hence

$$\tau = \frac{\log M}{M R_0} , \quad (7)$$

where the natural number e is taken as the basis of the "log" function. K_b in (5) can now be written as

$$K_b = \left(\frac{\lambda_0}{R_0}\right) \frac{\nu \log M}{ML} ,$$

where the ratio λ_0 / R_0 denotes the average background noise photons per nat time. We consider two different types of energy constraints on the laser source. The first type is average energy per pulse constraint, which is equivalent to $K_s / \nu =$ constant. The second type is average power constraint. This is equivalent to $K_s / T =$ constant or, using (7), $K_s / \log M =$ constant, i.e., fixed energy per information nat.

A. Fixed Energy per Pulse

In this part we study the effect of some system parameters on the performance (bit error rate) of optical PPM-CDMA systems under a constraint on the transmitted energy per pulse. This constraint is equivalent to fixed photon count per symbol (K_s). The product $\lambda_s T_c$ in (6) is thus equal to $\frac{K_s}{\nu}$, which denotes the average signal photon count

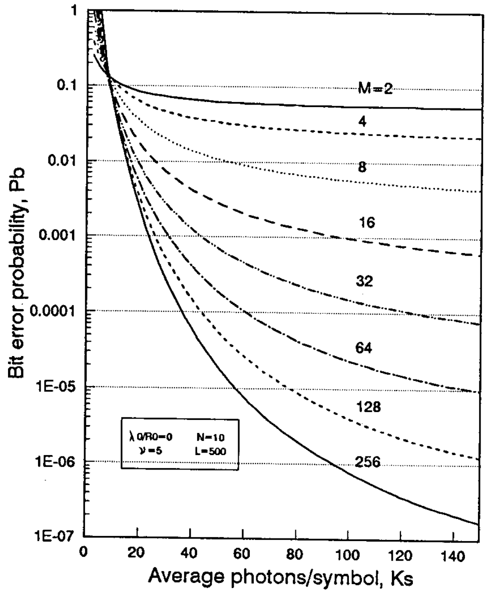

Fig. 3. Bit error probability versus average photons/symbol without background noise.

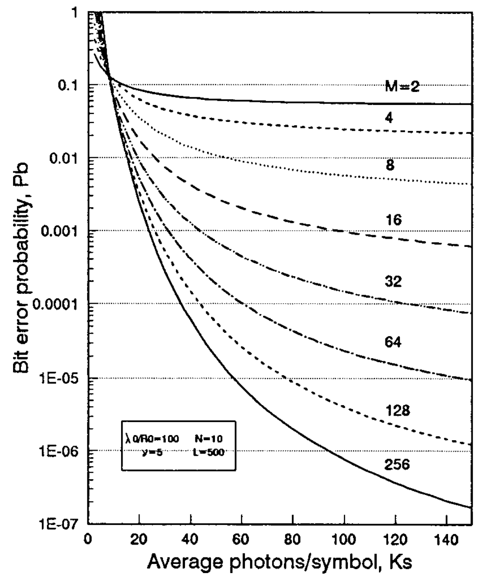

Fig. 4. Bit error probability versus average photons/symbol with background noise, $\lambda_0/R_0 = 100$.

per pulse. The bit error probability with $N = 10$, $\nu = 5$, and $L = 500$ has been evaluated and plotted in Figs. 3–5 for different values of K_s, M, and λ_0. In Fig. 3, the bit error rate is plotted under the assumption of zero background noise. In Fig. 4 and 5, however, the background noise has been assumed to be $\lambda_0/R_0 = 100$ and 500 photons/nat time, respectively. These figures display that the effect of the background noise on the performance is negligible. This indicates that the degradation in performance under same signal energy is mainly due to the multiple-user interference. Since the spreading code length (L) affects only the received background noise power, it has also a negligible effect on the performance. On the other hand, the effect of the pulse position multiplicity (M) and the code weight (ν) on the performance is remarkable. It is seen from Figs. 3–5 that the performance gets better as M increases. Moreover, this improvement is associated with a save in energy because the transmitted photons per nat ($K_s/\log M$) decreases as M increases. Fig. 6 demonstrates the effect of the code weight. It is seen from this figure that the performance gets worse when decreasing ν. Indeed, lowering ν will decrease the average signal energy with respect to the interference energy which leads to a more frequent wrong decisions and hence worse bit error rate.

B. Average Power Constraint

In this part we examine the performance of the above system under a constraint on the average power (or energy per information nat). Let μ denote the number of the transmitted photons per nat, K_s in (5) is now equal

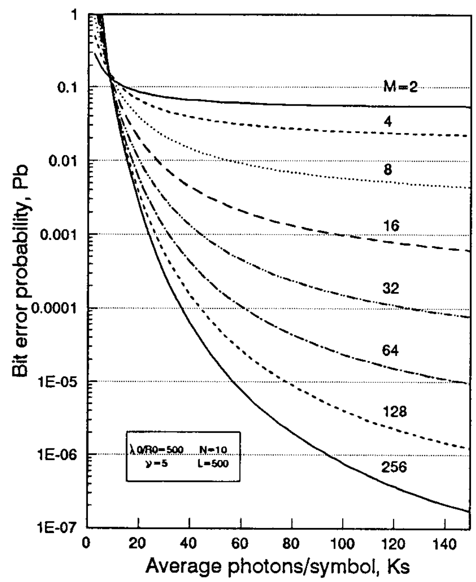

Fig. 5. Bit error probability versus average photons/symbol with background noise, $\lambda_0/R_0 = 500$.

to $K_s = \mu \log M$. Figs. 7 and 8 show the bit error rate versus the average photons per nat for a fixed number of users, weight, and chip size, and different values of M. As expected, when M increases, the system performance im-

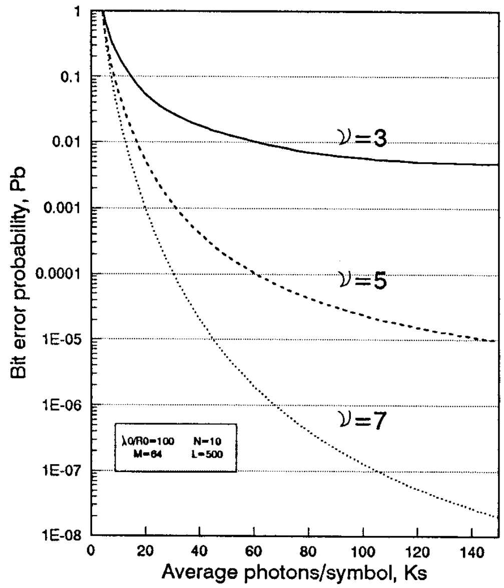

Fig. 6. Bit error probability versus average photons/symbol with background noise, $\lambda_0/R_0 = 100$.

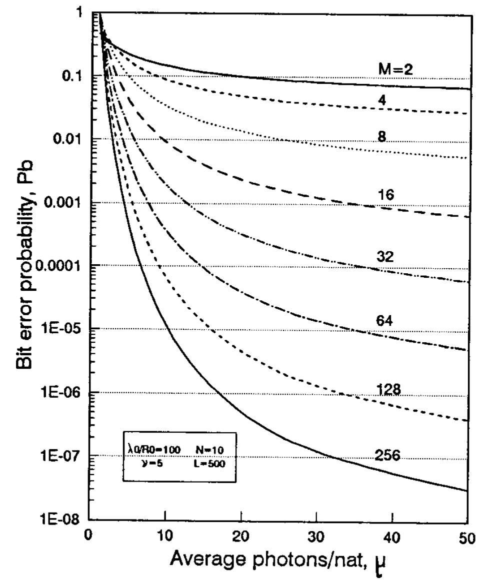

Fig. 7. Bit error probability versus average photons/nat with background noise, $\lambda_0/R_0 = 100$.

proves significantly. As an example, for a system with 10 users, weight/chip size of 5/500, background noise count of 100 photons/nat time, and signal energy of 50 photons/nat, the bit error rate equals 6.99×10^{-2} if $M = 2$, 6.7×10^{-4} if $M = 16$, and 3.21×10^{-8} if $M = 256$. The improve in this case is better than in case A because here the energy per pulse ($\mu \log M/\nu$) increases with M, however in case A the same energy per pulse (which is fixed) is used to transmit more information as M increases.

The effect of the maximum number of simultaneous users is explored in Figs. 9 and 10 under average energy per pulse and power constraints, respectively. Since we employ OOC's with auto- and cross-correlations that are bounded by one, the maximum number of subscribers is at most $\frac{L-1}{\nu(\nu-1)}$. As an example, consider a system with energy constraint of 30 photons/nat employing OOC's with $L = 500$ and $\nu = 5$. This system can accommodate at most 24 subscribers. Let the bit error rate be required to be less than 10^{-5}. From Fig. 9 (with $\lambda_0/R_0 = 100$) we see that systems with small values of M can not accommodate much simultaneous users. For example the number of users is at most 1, 2, or 4, when M equals 2, 4, or 16, respectively. If, on the other hand, $M = 64$, at most 9 users can communicate simultaneously and achieve the above error rate constraint. When $M = 256$, however, all the 24 subscribers can communicate reliably. The above example demonstrates that energy and bit error rate constraints may limit the maximum number of simultaneous users. However, increasing the value of the pulse position multiplicity may permit all the subscribers to communicate simultaneously. We explore in detail the relation between the number of simultaneous users and the pulse position multiplicity in the next section.

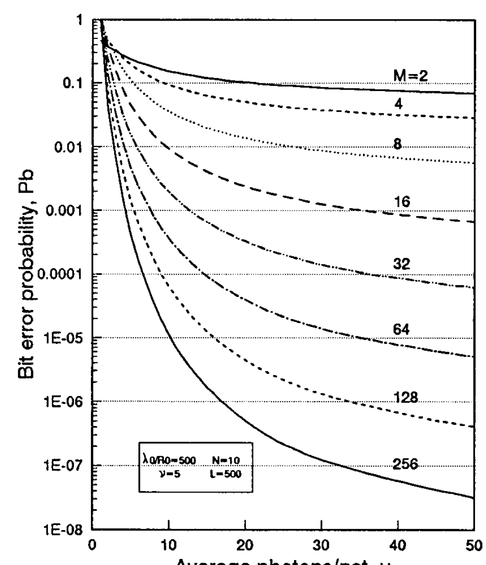

Fig. 8. Bit error probability versus average photons/nat with background noise, $\lambda_0/R_0 = 500$.

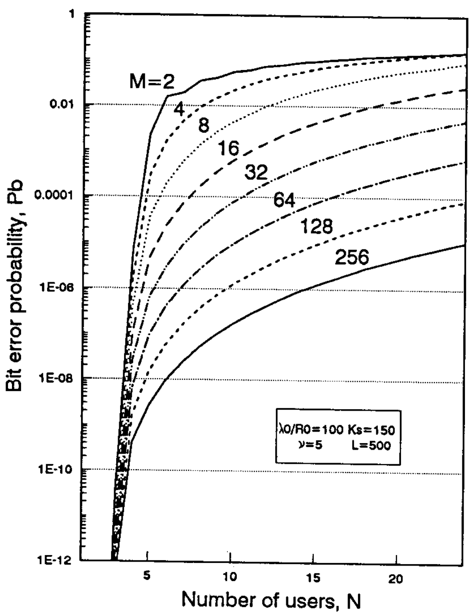

Fig. 9. Bit error probability versus the number of users for fixed energy of 150 photons/symbol.

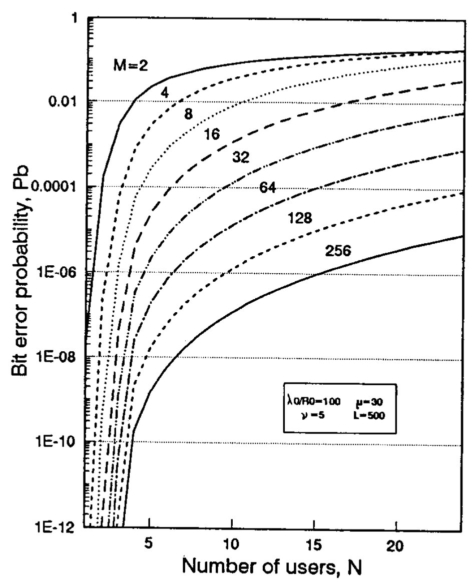

Fig. 10. Bit error probability versus the number of users for fixed energy of 30 photons/nat.

IV. Limits to the Maximum Number of Users (Asymptotic Results)

In this section we obtain an expression for the maximum number of users ($N_{M,\max}$) that can communicate simultaneously with asymptotically zero error rate. The asymptotic evaluation is for $M \to \infty$ with μ, ν, and L being fixed. We are able to show the following assertion:

$$\liminf_{M\to\infty} \frac{N_{M,\max} - 1}{M^{\frac{1+\rho\nu-e^{\rho}}{\rho\nu}}} \ge \nu e^{-(1+\rho)} ,$$

where $\rho \stackrel{\text{def}}{=} 1/\mu$ denotes the transmitted information in nats/photon. This indicates that, for ρ fixed, the maximum number of users can be increased as we wish by increasing the value of M as long as $1 + \rho\nu > e^{\rho}$ or

$$\nu > \frac{e^{\rho} - 1}{\rho} .$$

The main advantages of M-ary PPM-CDMA over OOK-CDMA are now obvious, where in the latter the maximum number of simultaneous users can not be increased without decreasing ρ (or increasing the average power) [2,6,7] to preserve a suitable bit error rate. Another advantage is that even if we increased the average power we still may not be able to accommodate all the subscribers in the case of OOK without degrading the performance. However for PPM we can accommodate *reliably* any number of users by increasing M. Of course the increase in system complexity is the new price that should be paid to gain the above advantages.

The proof of the above assertion is provided in Theorem 1 below. Before the proof of the theorem we develop (in Proposition 1) another upper bound on the probability of error. This bound is actually based on Chernoff inequality. In Appendix A we have introduced two lemmas that are essential to our derivations of both the proposition and the theorem.

Proposition 1: For any two real numbers $s \in [0,1]$ and $z \ge 1$, the probability of a word error, P_E, in the optical synchronous PPM-CDMA channel can be upper bounded as

$$-\frac{\log P_E}{\log M/\rho} \ge 1 - s\rho - z^{-s} - s\frac{\nu\lambda_0}{ML\lambda_a}\left(z - 1 - \frac{1-z^{-s}}{s}\right) + (N-1)\rho - \frac{(N-1)\rho}{\log M}\log\Big[(M-1)^{1-s} \times \left(M - 2 + M^{\frac{z-1}{\rho\nu}}\right)^s + M^{\frac{z^{-s}-1}{\rho\nu}}\Big] , \quad (8)$$

where $\lambda_a \stackrel{\text{def}}{=} \frac{K_s}{T} = \frac{\nu\lambda_s}{ML}$ denotes the average signal power.

Proof: We start by rewriting (3) as

$$P_C \ge \sum_l \Pr\{Y_0 > Y_1, \ldots, Y_{M-1} | b_0^1 = 0, \kappa = l\} \Pr\{\kappa = l\} ,$$

where l was defined previously as the vector $(l_0, \ldots, l_{M-1})$ and $\Pr\{Y_0 > Y_1, \ldots, Y_{M-1} | b_0^1 = 0, \kappa = l\}$ is given by (4). Hence

$$P_E = 1 - P_C \le \sum_l P[E|\kappa = l] \Pr\{\kappa = l\} ,$$

where

$$P[E|\kappa = l] \stackrel{\text{def}}{=} 1 - \Pr\{Y_0 > Y_1, \ldots, Y_{M-1} | b_0^1 = 0, \kappa = l\} = \sum_{k=0}^{\infty} e^{-(K_s+K_b+\lambda_s T_c l_0)} \frac{(K_s + K_b + \lambda_s T_c l_0)^k}{k!} \times \left[1 - \prod_{j=1}^{M-1}\left(1 - \sum_{i=k}^{\infty} e^{-(K_b+\lambda_s T_c l_j)} \frac{(K_b + \lambda_s T_c l_j)^i}{i!}\right)\right].$$

Notice that for any $s \in [0,1]$ and $x_j \in [0,1]$, $j \in \{0, \ldots, M-1\}$,

$$1 - \prod_{j=1}^{M-1}(1 - x_j) \le \left(1 - \prod_{j=1}^{M-1}(1 - x_j)\right)^s \le \left(\sum_{j=1}^{M-1} x_j\right)^s,$$

where we have used Lemma 1, Appendix A, to justify the last inequality. Hence

$$P[E|\kappa = l] \le \sum_{k=0}^{\infty} e^{-(K_s+K_b+\lambda_s T_c l_0)} \frac{(K_s + K_b + \lambda_s T_c l_0)^k}{k!} \times \left[\sum_{j=1}^{M-1} \sum_{i=k}^{\infty} e^{-(K_b+\lambda_s T_c l_j)} \frac{(K_b + \lambda_s T_c l_j)^i}{i!}\right]^s. \quad (9)$$

Making use of Chernoff inequality, we obtain, for any $z \ge 1$,

$$\sum_{i=k}^{\infty} e^{-(K_b+\lambda_s T_c l_j)} \frac{(K_b + \lambda_s T_c l_j)^i}{i!} \le \sum_{i=k}^{\infty} z^{i-k} e^{-(K_b+\lambda_s T_c l_j)} \frac{(K_b + \lambda_s T_c l_j)^i}{i!} \le z^{-k} \sum_{i=0}^{\infty} z^i e^{-(K_b+\lambda_s T_c l_j)} \frac{(K_b + \lambda_s T_c l_j)^i}{i!} = z^{-k} \exp[(K_b + \lambda_s T_c l_j)(z-1)].$$

Substituting in (9), yields

$$P[E|\kappa = l] \le \exp[(K_s + K_b + \lambda_s T_c l_0)(z^{-s} - 1)] \times \left[\sum_{j=1}^{M-1} \exp[(K_b + \lambda_s T_c l_j)(z-1)]\right]^s.$$

Thus we can write

$$P_E \le \sum_l P[E|\kappa = l] \Pr\{\kappa = l\} \le \sum_{l_0} \Pr\{\kappa_0 = l_0\} \times \exp[(K_s + K_b + \lambda_s T_c l_0)(z^{-s} - 1)] \times \sum_{l_1^{M-1}} \Pr\{\kappa_1^{M-1} = l_1^{M-1} | \kappa_0 = l_0\} \times \left[\sum_{j=1}^{M-1} \exp[(K_b + \lambda_s T_c l_j)(z-1)]\right]^s,$$

where $\kappa_1^{M-1} \stackrel{\text{def}}{=} (\kappa_1, \ldots, \kappa_{M-1})$ and $l_1^{M-1} \stackrel{\text{def}}{=} (l_1, \ldots, l_{M-1})$. Using the concavity of the function x^s, any $s \in [0,1]$, we obtain

$$P_E \le \sum_{l_0} \Pr\{\kappa_0 = l_0\} \exp[(K_s + K_b + \lambda_s T_c l_0)(z^{-s} - 1)] \times \left[\sum_{j=1}^{M-1} \sum_{l_j} \Pr\{\kappa_j = l_j | \kappa_0 = l_0\} \times \exp[(K_b + \lambda_s T_c l_j)(z-1)]\right]^s \le (M-1)^s \sum_{l_0=0}^{N-1} \Pr\{\kappa_0 = l_0\} \times \exp[(K_s + K_b + \lambda_s T_c l_0)(z^{-s} - 1)] \times \left[\sum_{l_1=0}^{N-1-l_0} \Pr\{\kappa_1 = l_1 | \kappa_0 = l_0\} \times \exp[(K_b + \lambda_s T_c l_1)(z-1)]\right]^s.$$

The last summation can be evaluated as follows

$$\sum_{l_1=0}^{N-1-l_0} \Pr\{\kappa_1 = l_1 | \kappa_0 = l_0\} \times \exp[(K_b + \lambda_s T_c l_1)(z-1)] = \sum_{l_1=0}^{N-1-l_0} \binom{N-1-l_0}{l_1} \left(\frac{1}{M-1}\right)^{l_1} \left(\frac{M-2}{M-1}\right)^{N-1-l_0-l_1} \times \exp[(K_b + \lambda_s T_c l_1)(z-1)] = e^{K_b(z-1)} \left[1 + \frac{e^{\lambda_s T_c(z-1)} - 1}{M-1}\right]^{N-1-l_0}.$$

Thus

$$P_E \le (M-1)^s \exp[sK_b(z-1)] \times \sum_{l_0=0}^{N-1} \binom{N-1}{l_0} \left(\frac{1}{M}\right)^{l_0} \left(1 - \frac{1}{M}\right)^{N-1-l_0} \times \exp[(K_s + K_b + \lambda_s T_c l_0)(z^{-s} - 1)] \times \left[1 + \frac{e^{\lambda_s T_c(z-1)} - 1}{M-1}\right]^{s(N-1-l_0)} = (M-1)^s \exp[K_s(z^{-s} - 1) + K_b(z^{-s} - 1) + sK_b(z-1)] \times \left[\frac{e^{\lambda_s T_c(z^{-s}-1)}}{M} + \frac{(M-2+e^{\lambda_s T_c(z-1)})^s}{(M-1)^{s-1}M}\right]^{N-1}.$$

Taking the logarithm with base e and arranging the terms, yields

$$-\log P_E \ge -s\log(M-1) - K_s(z^{-s} - 1) - K_b(z^{-s} - 1) - sK_b(z-1) + (N-1)\log M - (N-1)\log\left[(M-1)^{1-s}(M-2+e^{\lambda_s T_c(z-1)})^s + e^{\lambda_s T_c(z^{-s}-1)}\right].$$

By substituting $K_s = \frac{\log M}{\rho}$, $K_b = \frac{\log M}{\rho}\frac{\nu\lambda_0}{ML\lambda_a}$, and $\lambda_s T_c = \frac{\log M}{\rho\nu}$ and rearranging the terms we get

$$-\frac{\log P_E}{\log M/\rho} \geq 1 - s\rho - z^{-s} - s\frac{\nu\lambda_0}{ML\lambda_a}\left(z - 1 - \frac{1-z^{-s}}{s}\right) + (N-1)\rho - \frac{(N-1)\rho}{\log M}\log\left[(M-1)^{1-s} \times \left(M - 2 + M^{\frac{z-1}{\rho\nu}}\right)^s + M^{\frac{z^{-s}-1}{\rho\nu}}\right]. \qquad \square$$

Theorem 1: For optical orthogonal code sequences with weight ν and cross-correlations bounded by one, the maximum number of simultaneous users, in the optical synchronous PPM-CDMA system, is lower bounded by

$$\liminf_{M\to\infty} \frac{N_{M,\max} - 1}{M^{\frac{1+\rho\nu-e^\rho}{\rho\nu}}} \geq \nu e^{-(1+\rho)},$$

where ρ and M denote the transmitted information in nats per photon and the pulse position multiplicity, respectively.

Remark 1: If $1 + \rho\nu > e^\rho$, then $N_{M,\max}$ can be increased without limit by increasing M. The maximum number of the available OOC's and/or system synchronization problems, however, will limit $N_{M,\max}$.

Remark 2: One can easily see that the inequality in the above remark remains true by setting $\rho = \log\nu$. This means that the channel capacity, C_{ph} (in nats per photon), of the optical PPM-CDMA channel can be lower bounded by

$$C_{ph} \geq \log\nu.$$

Remark 3: In the following proof we will ignore the effect of the background noise, ($\lambda_0 = 0$). With minor modifications in the proof, however, it is easy to check that the above assertion remains unchanged if we take the background noise into account.

Proof: We start by estimating suitable values of $s \in [0, 1]$ and $z \geq 1$ for the upper bound given in Proposition 1 so as to have asymptotically zero error rate. In fact if we show that the right hand side of (8) is positive (i.e., greater than some $\delta > 0$) then we get $P_E \leq \exp[-\frac{\log M}{\rho}\delta] \to 0$ as $M \to \infty$. Let $h(s,z) \stackrel{\text{def}}{=}$ the right hand side of (8). From the continuity of the function $h(s,z)$, we notice that

$$h(s,z) = \left[\lim_{s\to 0}\frac{1}{s}h(s,z) - o(s)\right]s,$$

where $o(s) \to 0$ as $s \to 0$. Hence for s arbitrary small $h(s,z) > 0$ if $\lim_{s\to 0}\frac{1}{s}h(s,z) > 0$. It is easy to check that

$$\lim_{s\to 0}\frac{1}{s}h(s,z) = \log z - \rho - \frac{\nu\lambda_0}{L\lambda_a}\cdot\frac{z-1-\log z}{M} - \frac{(N-1)\rho}{\log M} \times \frac{(M-1)\log\frac{M-2+M^{\frac{z-1}{\rho\nu}}}{M-1} - \frac{\log M}{\rho\nu}\log z}{M}.$$

Assuming zero background noise, $\lambda_0 = 0$, the last equation simplifies to

$$\lim_{s\to 0}\frac{1}{s}h(s,z) = \log z - \rho - \frac{(N-1)\rho}{\log M} \times \frac{(M-1)\log\frac{M-2+M^{\frac{z-1}{\rho\nu}}}{M-1} - \frac{\log M}{\rho\nu}\log z}{M}.$$

We provide a lower bound on the above function limit:

$$\begin{aligned}\lim_{s\to 0}\frac{1}{s}h(s,z) &\geq \log z - \rho - \frac{(N-1)\rho}{\log M}\cdot\frac{M-1}{M} \times \log\frac{M-2+M^{\frac{z-1}{\rho\nu}}}{M-1} \\ &\geq \log z - \rho - \frac{(N-1)\rho}{\log M}\cdot\frac{M-1}{M}\cdot\frac{M^{\frac{z-1}{\rho\nu}}-1}{M-1} \\ &\geq \log z - \rho - \frac{(N-1)\rho}{\log M}M^{\frac{z-1-\rho\nu}{\rho\nu}},\end{aligned}$$

where we have made use of the facts that $z \geq 1$ and $\log(1+x) \leq x$ in the first and second inequalities, respectively. The last term is positive if

$$N - 1 < \frac{\log z - \rho}{M^{\frac{z-1-\rho\nu}{\rho\nu}}\frac{\rho}{\log M}}$$

for every $z \geq 1$. Hence

$$N_{M,\max} - 1 \geq \max_{z\geq 1}\frac{\log z - \rho}{M^{\frac{z-1-\rho\nu}{\rho\nu}}\frac{\rho}{\log M}}.$$

Define the function

$$f(z) \stackrel{\text{def}}{=} \frac{\log z - \rho}{M^{\frac{z-1-\rho\nu}{\rho\nu}}\frac{\rho}{\log M}}. \tag{10}$$

Thus $N_{M,\max} - 1 \geq \max_{z\geq 1} f(z)$. To obtain the maximum of $f(z)$ we differentiate this function with respect to z and equate the result with zero. Hence the optimizing z^* must satisfy

$$(z^*)^{-1} - (\log z^* - \rho)\frac{\log M}{\rho\nu} = 0 \tag{11}$$

or using Lemma 2, Appendix A,

$$e^\rho \leq z^* \leq e^\rho + \frac{\rho\nu}{\log M}. \tag{12}$$

From (10) and (11), we obtain

$$N_{M,\max} - 1 \geq \frac{\nu}{z^* M^{\frac{z^*-1-\rho\nu}{\rho\nu}}}.$$

Making use of (12), we get further the lower bound

$$\begin{aligned}N_{M,\max} - 1 &\geq \frac{\nu}{\left(e^\rho + \frac{\rho\nu}{\log M}\right)M^{\frac{e^\rho-1-\rho\nu}{\rho\nu}+\frac{1}{\log M}}} \\ &= \frac{\nu e^{-1}}{\left(e^\rho + \frac{\rho\nu}{\log M}\right)M^{\frac{e^\rho-1-\rho\nu}{\rho\nu}}}.\end{aligned}$$

Whence

$$\frac{N_{M,\max}-1}{M^{\frac{1+\rho\nu-e^\rho}{\rho\nu}}} \geq \frac{\nu e^{-1}}{e^\rho + \frac{\rho\nu}{\log M}} . \qquad \square$$

V. Extensions and Concluding Remarks

Direct-detection optical synchronous CDMA systems with PPM signaling has been studied in details. We considered optical orthogonal codes, with cross-correlations bounded by one, as the signature code sequences in our system. The Poisson shot noise model has been assumed for the receiver photodetector. The background noise and multiple-user interference have been accounted for in estimating the bit error rate. In our numerical evaluation we derived a union upper bound on the probability of error to simplify the calculations. We have evaluated the performance under the restriction of fixed throughput rate. We can thus extract the following concluding remarks.

i) Under fixed photon energy per symbol, the performance (bit error rate) of the system improves as M increases. Furthermore, the average power and the total energy are reduced by a factor $\log 2/\log M$ times that required in binary PPM-CDMA.
ii) Under fixed photon energy per information nat, the performance improves significantly (as expected) as M increases. The improve in this case is better than in (i) because here the energy per pulse increases with M, however in case (i) the same energy per pulse is used to transmit more information as M increases with bit rate held fixed.
iii) Under average power and bit error rate constraints, a pulse position multiplicity $M_1 > 0$ always exists so that if $M \geq M_1$, all the subscribers can communicate simultaneously.

In the last part of the paper, another upper bound on the probability of error has also been obtained with the aid of Chernoff inequality. This bound has been used to derive an expression for the maximum number of simultaneous users that can communicate with asymptotically zero error rate. It has been shown that this number increases *asymptotically* with M as long as $\nu > \frac{e^\rho-1}{\rho}$. This fact supports our conclusion (iii) because we can increase M as we wish and in turn N_M. However, N_M can not increase without limit because it is bounded by the maximum number of codes which is at most $\frac{L-1}{\nu(\nu-1)}$.

Two main advantages of PPM-CDMA over OOK-CDMA are remarked:

i) Under bit error rate constraint, the maximum number of simultaneous users can not be increased, in the case of OOK-CDMA, without increasing the average power. In the case of PPM-CDMA, however, we can increase this number by increasing M and preserving the average power fixed.
ii) Even if we increased the average power we still may not be able to accommodate all the subscribers in the case of OOK. However for PPM, as mentioned in (iii) above, we can accommodate any number of users by increasing M. The reason is that, for OOK, the *average* number of interfering optical pulses equals $\frac{N-1}{2}$. This average number reduces to $\frac{N-1}{M}$ for PPM.

Of course these advantages are obtained at the expense of increasing the system complexity.

To increase the maximum number of codes, we can use OOC's with cross-correlations that are bounded by two [8,11], where we can get $\frac{(L-1)(L-2)}{\nu(\nu-1)(\nu-2)}$ codes. In this case, the maximum number simultaneous of users that can communicate with asymptotically zero error rate can be shown to be bounded by

$$\liminf_{M\to\infty} \frac{N_{M,\max}-1}{M^{\frac{1+\rho\nu/2-e^\rho}{\rho\nu/2}}} \geq \frac{\nu}{2} e^{-(1+\rho)} .$$

Our results in Section IV can easily be extended to asynchronous CDMA. In this case the assertion in Theorem 1 would be modified to

$$\liminf_{M\to\infty} \frac{N_{M,\max}-1}{M^{\frac{1+\rho\nu-e^\rho}{\rho\nu}}} \geq \frac{L}{\nu} e^{-(1+\rho)} .$$

The proof is pretty much similar to the one provided in the paper with slight modifications.

Appendix A

Lemma 1: Let $x_i \in [0,1]$, $i \in \{0,1,\ldots,M-1\}$, where M is any positive integer. Then

$$\prod_{i=0}^{M-1}(1-x_i) \geq 1 - \sum_{i=0}^{M-1} x_i .$$

Proof: Let the function $f\colon [0,1]^M \mapsto \mathbf{R}$ be defined as follows:

$$f(x) \stackrel{\text{def}}{=} \prod_{i=0}^{M-1}(1-x_i) + \sum_{i=0}^{M-1} x_i - 1 .$$

It suffices to show that $f(x) \geq 0$ or $\min_{x\in[0,1]^M} f(x) = 0$. Notice that, for any $k \in \{0,\ldots,M-1\}$,

$$\begin{aligned}\min_{x_k\in[0,1]} f(x) &= \min_{x_k\in[0,1]} \Bigg[x_k\Bigg(1 - \prod_{\substack{i=0,\\ i\neq k}}^{M-1}(1-x_i)\Bigg) \\ &\qquad + \prod_{\substack{i=0,\\ i\neq k}}^{M-1}(1-x_i) + \sum_{\substack{i=0,\\ i\neq k}}^{M-1} x_i - 1\Bigg] \\ &= \prod_{\substack{i=0,\\ i\neq k}}^{M-1}(1-x_i) + \sum_{\substack{i=0,\\ i\neq k}}^{M-1} x_i - 1 ,\end{aligned}$$

where the last equality is achieved for $x_k = 0$ (since $\prod_{\substack{i=0,\\ i\neq k}}^{M-1}(1-x_i) \leq 1$). Since k was arbitrary, we conclude that the minimum occurs at $x = 0^M$. Hence $\min_{x\in[0,1]^M} f(x) = f(0^M) = 0$. □

Lemma 2: Consider the function

$$g(z) \stackrel{\text{def}}{=} z^{-1} - (\log z - \rho)\frac{\log M}{\rho\nu}\,, \qquad z \geq 1$$

where M and ν are positive integers, and $\rho > 0$. The solution of the equation $g(z) = 0$ must satisfy the inequalities:

$$e^{\rho} \leq z \leq e^{\rho} + \frac{\rho\nu}{\log M}\,.$$

Proof: This function is monotonically decreasing in z as long as $z \geq 1$. Indeed since the first derivative of $g(\cdot)$ is negative:

$$(\forall z \geq 1) \qquad \frac{dg}{dz}(z) = -z^{-2} - \frac{\log M}{\rho\nu}z^{-1} < 0\,.$$

Hence it suffices to show that

$$g(e^{\rho}) \geq 0 \qquad \text{and} \qquad g(e^{\rho} + \frac{\rho\nu}{\log M}) \leq 0\,.$$

Indeed, we have

$$g(e^{\rho}) = e^{-\rho} > 0$$

and

$$\begin{aligned} g(e^{\rho} + \frac{\rho\nu}{\log M}) &= \frac{1}{e^{\rho} + \frac{\rho\nu}{\log M}} \\ &\quad - \frac{\log M}{\rho\nu}\left[\log\left(e^{\rho} + \frac{\rho\nu}{\log M}\right) - \rho\right] \\ &= \frac{1}{e^{\rho} + \frac{\rho\nu}{\log M}} - \frac{\log M}{\rho\nu}\log\left(1 + \frac{\rho\nu}{\log M}e^{-\rho}\right) \\ &\leq \frac{1}{e^{\rho} + \frac{\rho\nu}{\log M}} - \frac{\log M}{\rho\nu}\,\frac{\frac{\rho\nu}{\log M}e^{-\rho}}{1 + \frac{\rho\nu}{\log M}e^{-\rho}} = 0\,, \end{aligned}$$

where we have made use of the fact that $\log y \geq 1 - 1/y$ to justify the last inequality. □

References

[1] G. Vannucci and S. Yang, "Experimental spreading and despreading of the optical spectrum," *IEEE Trans. Commun.*, vol. COM-37, pp. 777–780, July 1989.

[2] J. A. Salehi, "Code division multiple-access techniques in optical fiber networks–Part I: Fundamental principles," *IEEE Trans. Commun.*, vol. COM-37, pp. 824–833, Aug. 1989.

[3] J. A. Salehi and C. A. Brackett, "Code division multiple-access techniques in optical fiber networks–Part II: Systems performance analysis," *IEEE Trans. Commun.*, vol. COM-37, pp. 834–842, Aug. 1989.

[4] W. C. Kwong, P. A. Perrier, and P. R. Prucnal, "Performance comparison of asynchronous and synchronous code-division multiple-access," *IEEE Trans. Commun.*, vol. COM-39, pp. 1625–1634, Nov. 1991.

[5] D. J. Hajela and J. A. Salehi, "Limits to the encoding and bounds on the performance of coherent ultrashort light pulse code-division multiple-access systems," *IEEE Trans. Commun.*, vol. COM-40, pp. 325–336, Feb. 1992.

[6] A. W. Lam and A. M. Hussain, "Performance analysis of direct-detection optical CDMA communication systems with avalanche photodiodes," *IEEE Trans. Commun.*, vol. COM-40, pp. 810–820, Apr. 1992.

[7] M. Dale and R. M. Gagliardi, "Analysis of fiberoptic code-division multiple access," Univ. Southern Calif., CSI Tech. Rep. 92-06-10, Jun. 1992.

[8] M. Azizoğlu, J. A. Salehi, and Y. Li, "Optical CDMA via temporal codes," *IEEE Trans. Commun.*, vol. COM-40, pp. 1162–1170, July 1992.

[9] D. Brady and S. Verdú, "A semiclassical analysis of optical code division multiple access," *IEEE Trans. Commun.*, vol. COM-39, pp. 85-93, Jan. 1991.

[10] F. R. K. Chung, J. A. Salehi, and V. K. Wei, "Optical orthogonal codes: Design, analysis, and applications," *IEEE Trans. Inform. Theory*, vol. IT-35, pp. 595–604, May 1989.

[11] H. Chung and P. V. Kumar, "Optical orthogonal codes–new bounds and an optimal construction," *IEEE Trans. Inform. Theory*, vol. IT-36, pp. 866–873, July 1990.

[12] K. P. Jackson, S. A. Newton, B. Moslehi, M. Tur, C. C. Culter, J. W. Goodman, and H. J. Show, "Optical fiber delay-line signal processing," *IEEE Trans. Microwave Theory Technol.*, vol. MTT-33, pp. 193–210, Mar. 1985.

[13] R. M. Gagliardi and S. Karp, *Optical Communications.* New York: John Wiley, 1976.

[14] J. R. Pierce, "Optical channels: Practical limits with photon counting," *IEEE Trans. Commun.*, vol. COM-26, pp. 1819–1821, Dec. 1978.

[15] J. L. Massey, "Capacity, cutoff rate, and coding for a direct-detection optical channel," *IEEE Trans. Commun.*, vol. COM-29, pp. 1615-1621, Nov. 1981.

Hossam M. H. Shalaby (S'83–M'91) was born in Giza, Egypt in 1961. He received his B.S. and M.S. degrees in electrical engineering from the University of Alexandria, Egypt in 1983 and 1986, respectively, and the Ph.D. degree in electrical engineering in 1991 from the University of Maryland, College Park.

He is currently an Assistant Professor at the Faculty of Engineering, University of Alexandria, Egypt. His research interests are in communication theory, optical communications, signal detection and estimation, and information theory.

Dr. Shalaby was a recipient of an SRC fellowship 1987-1991.